Supporting Information

Quantitation of affinity, avidity, and binding kinetics of protein analytes with a dynamically switchable biosurface

Jelena Knezevic, Andreas Langer, Paul A. Hampel, Wolfgang Kaiser, Ralf Strasser, Ulrich Rant*

Walter Schottky Institute & Institute for Advanced Study, Technische Universität München, 85748 Garching, Germany

* rant@tum.de

Contents

1 Materials and Methods

Triaminated 48mer DNA used for the cDNA-trisNTA conjugation was obtained from Integrated DNA Technologies, USA (5' /5AmMC6//iUniAmM//iUniAmM/ATC AGC GTT CGA TGC TTC CGA CTA ATC AGC CAT ATC AGC TTA CGA CTA 3'= cDNA-$(NH_2)_3$). /5AmMC6/and /iUniAmM/ are IDT codes for the 5' amino modification and internal amino modification of DNA, respectively. All other sequences (48 mers) have been obtained from IBA GmbH, Germany (5' HS-(CH2)6-TAG TCG TAA GCT GAT ATG GCT GAT TAG TCG GAA GCA TCG AAC GCT GAT-Cy3 3' (HS-ssDNA-Cy3) and 5' ATC AGC GTT CGA TGC TTC CGA CTA ATC AGC CAT ATC AGC TTA CGA CTA 3' (cDNA-x)).

His_6 tagged proteins A, G and L were obtained from BioCat, Germany. His_6-myelin oligodendrocyte glycoprotein (MOG) was obtained from Abcam, UK. His_6-interferon alpha (INFα) was provided by Qiagen, Germany. His_6-Fab fragment (Fab) was provided by MorphoSys AG, Germany. Protein A features one His_6 tag at the N-terminal and one at the C-terminal. All other aforementioned proteins feature one N-terminal His_6 tag.

Buffer compounds were purchased from Sigma Aldrich and from Carl Roth, Germany. N-succinimidyl 3-(2-pyridyldithio) propionate (SPDP), dimethyl sulfoxide (DMSO) and Tris(2-carboxyethyl)phosphine hydrochloride (TCEP) were obtained from SIGMA Aldrich, Germany. Maleimido-C3-NTA was obtained from Dojindo, Japan.

1.1 Conjugation of cDNA with trisNTA

cDNA-trisNTA conjugation was carried out by following the protocol of Goodman et al. [1] with minor changes. 0.2 mM triaminated DNA was incubated with the 125-fold molar excess of SPDP[1] freshly solved in DMSO for one hour at room temperature (final DNA concentration 0.16 mM). The N-hydroxysuccinimid (NHS) ester of SPDP reacts with the amino group of the DNA linker, forming stable amide bonds. A 3 kDa MW cutoff filter (Amicon Ultra, Millipore) was used to remove excess SPDP and exchange the solvent with the reaction buffer (0.1 M PBS, 0.15 M NaCl, pH 7.3). The disulfide bridges of SPDP molecules were then reduced by incubating the collected sample in the freshly prepared 60-fold molar excess of TCEP[2] for 30 min. 100 mM Maleimido-C3-NTA solution was prepared by dissolving Maleimido-C3-NTA in reaction buffer. A 70-fold molar excess of maleimido-C3-NTA was mixed to the sample and incubated at RT over the night. Finally, the solvent was exchanged with the standard buffer solution (10 mM Tris, 50 mM NaCl, pH=7.4) using a 3 kDa MW cutoff filter (Amicon Ultra). Reaction products were analyzed by mass spectrometry (MALDI TOF) and reverse phase liquid chromatography (Figure S 1).

[1] SPDP stock concentration: 100 mM

[2] TCEP stock concentration: 100 mM

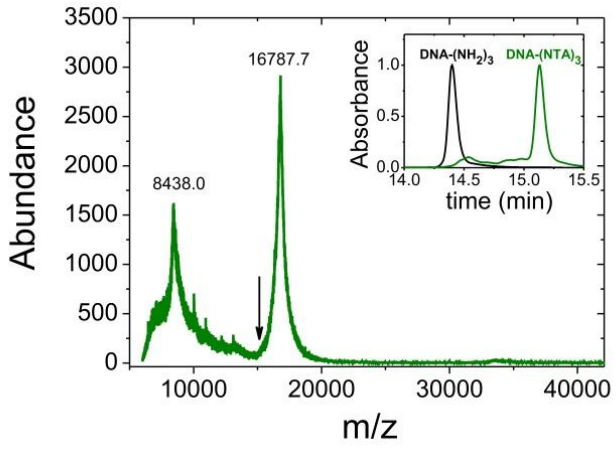

Figure S 1 Mass spectrum of cDNA-trisNTA conjugates. The molecular weight of cDNA-trisNTA conjugates with deprotonated carboxyl groups is expected to be 16 781.6 Da. The molecular weight of triaminated DNA is expected to be 15 244.1 Da (indicated by black arrow). Inset: RPLC chromatogram at 260nm of triaminated DNA (black line) and cDNA-trisNTA conjugates (green line) at 2% acetonitrile min^{-1} gradient (Agilent ZORBAX 300SB-C18 column).

The pronounced MS peak at 16787.7 can be attributed to cDNA-trisNTA conjugates, which have an expected molecular weight of 16 781.6 Da (with deprotonated carboxyl groups). cDNA-trisNTA conjugates were also analyzed by RPLC, monitoring the absorbance at 260 nm while the sample (cDNA-$(NH_2)_3$ or cDNA-trisNTA) was eluted from the column using an elution gradient of 2% acetonitrile min^{-1}. In order to evaluate the conjugation yield, the integrated area of the cDNA-trisNTA conjugate peak was compared to the total integrated area, suggesting that the sample contained at least 75% cDNA-trisNTA conjugates.

1.2 Measurement setup

Gold and platinum electrodes were deposited on 2 inch glass or sapphire wafers by optical lithography and standard vapor deposition techniques (thermal and electron beam evaporation). Flow cells were formed by clamping silicon O-rings in the opening of the intermediate plate positioned between the substrate wafer and the cover plate (Topas®). A Peltier element integrated in the sample holder enables temperature controlled experiments. External electric signals regulated by a data acquisition (DAQ) card are applied to the working gold electrode with respect to a reference platinum electrode. An integrated oscilloscope was used to measure electrode charging currents.

A green LED was used for the excitation of the Cy3 fluorescence light. The LED light was filtered by a 517 nm band pass filter and coupled via a dichroic mirror into a 50x microscope objective. Emitted Cy3 fluorescence light (570nm) was collected by the same microscope objective, passed through the dichroic mirror, a long pass filter, and was detected by a photomultiplier connected to a single photon counting unit. A time-correlated multichannel photon counting system was triggered by the falling edge of the electrical AC square-wave signal applied to the gold electrode and used to record the photon arrival time with 32 ns resolution.

1.3 DNA layer preparation and regeneration

Prior to the DNA immobilization on the gold electrodes, wafers were cleaned in freshly prepared Piranha solution (95% H_2SO_4 :30% H_2O_2 = 2:1) and HNO_3 (60%) for 15 minutes, each time followed by extensive rinsing with deionized water and 3 min sonication. After drying with nitrogen gas, electrodes were spotted with droplets of 1 µM DNA solution (10 mM Tris, 200 mM NaCl, pH=7.4) by using piezo-driven picoliter dispenser in non-contact mode (Autodrop Pipette AD-K-501 from Microdrop, Germany). In order to prevent drying of the spotted DNA solution and ensure a homogeneous surface density of the monolayer, the immobilization procedure was carried out in glove box at ambient humidity of 80%. For preparation of DNA-trisNTA layers, ssDNA solution (1 µM HS-ss48-Cy3, 10 mM Tris, 200 mM NaCl) was spotted on the gold surface as described above. Reference DNA layers were prepared by

immobilizing dsDNA, which was hybridized in solution from ssDNA with an excess of the complementary DNA (20 µM HS-ssDNA-Cy3, 27 µM cDNA-x, 10 mM Tris, 200 mM NaCl, pH=7.4). The DNA solution was heated up to 60 °C and slowly cooled down to RT. For spotting, 20 µM dsDNA solution was then diluted to 1 µM DNA (10 mM Tris, 200 mM NaCl, pH=7.4).

After installing the wafer in the flow cell, the electrodes were exposed to 1 mM 6-mercapto-1-hexanol (MCH) solution. MCH molecules displace nonspecifically bound DNA and passivate the remaining electrode surface [2, 3]. Due to the passivation step, both electrodes, Au and Pt exhibit characteristics of ideally polarizable electrodes without faradaic current flow. The final DNA surface density was adjusted by controlled electrical desorption, as described previously [4]. By applying sufficiently negative potentials in the range of -0.6 V to -1.0 V (vs. Pt), Au-S bonds are reduced. Before and after each desorption cycle, the surface density of the DNA layer was analyzed by evaluating the relative fluorescence modulation amplitude. To this end, electric potentials were switched at 0.2 Hz between typically +0.4 V and –0.4 V, while the fluorescence modulation amplitude was monitored in real-time. At high surface densities, steric interaction hinders DNA molecules to lie down completely and low modulation amplitudes are observed. As the surface density decreases, steric hindrances lessen and the *relative* fluorescence modulation amplitude (= absolute modulation amplitude divided by the fluorescence signal of a standing DNA layer, i.e., at negative bias) increases. The maximal value of the relative fluorescence modulation amplitude corresponds to the surface density where all DNA molecules can lie down completely [5]. Surface densities have been adjusted to be of the order of 10^{10} molecules/cm². An electrochemical quantitation method [6] confirmed that the DNA surface density was below 10^{11} molecules/cm², which is the approximate detection limit of this method. Finally, ssDNA layers were hybridized with 50 nM cDNA-trisNTA solution (10 mM Tris, 50 mM NaCl, pH=7.4, incubation time ≥ 30min). Complete hybridization of the DNA layer was confirmed by observing as a saturation of the relative fluorescence modulation amplitude, as described in [4, 7]. If required, additional electric desorption steps were carried out to adjust even lower surface densities of the dsDNA-trisNTA layer. The regeneration of DNA layers was carried out in two steps. First, double stranded DNA was denatured with 10 mM NaOH (3 min, continuous flow 0.05 ml/min). After rinsing buffer solution over the sensors surface for 5 min, the remaining single stranded DNA layers were hybridized again with fresh 50 nM DNA solution of the desired cDNA sequence (with or without tris-NTA, 10 mM Tris, 50 mM NaCl, pH=7.4, hybridization time ~1/2 h). Finally, excess cDNA was washed out by rinsing standard buffer solution over the sensor surface for approximately 15 min.

1.4 Nickel loading of trisNTA

Different multivalent ions can be used to bind His_6-tagged proteins to NTA compounds. Ni^{2+} ions are commonly used, since they are known to form very stable chelates with NTA (Cu^{2+}>Ni^{2+}>Zn^{2+}>>Ca^{2+}, Mg^{2+}) [8]). In order to achieve a homogenous Ni^{2+} loading of trisNTA, prior to the each loading step 5 mM EDTA solution[3] was flowed (0.05 ml/min) over the sample for 10 min prior to each loading step to remove other multivalent ions (trace impurities in the buffer solution). After reducing the EDTA concentration to 50 µM, trisNTA molecules were loaded with Ni^{2+} ions by flowing 500 µM $NiCl_2$ solution[4] over the sensor surface for 10 min. The number of NTA molecules per electrode is 5-50 pmol (assuming a surface density of DNA layer to be 10^{10}-10^{11} molecules/cm²). It is expected that each NTA moiety is loaded with one Ni^{2+} ion (no sharing), since a high excess of Ni^{2+} ions was used and the NTA-Ni^{2+} interaction is energetically preferred over the NTA-Ni^{2+}-NTA interaction [9]. Finally, the surface was rinsed thoroughly to wash out excess Ni^{2+} ions.

1.5 DNA layer characterization

Before and after each protein binding cycle, (i) the steady state conformation (orientation) of the DNA layers as a function of applied DC potentials, and (ii) the dynamic response when switching the electrode potential from positive to negative values, were measured.. In addition, the electrode charging current was recorded.

[3] solved in 10 mM Tris, 50 mM NaCl, pH≈7.4
[4] 500 µM $NiCl_2$, 10 mM Tris, 50 mM NaCl, pH≈7.4

For (i), DC potentials were applied to the gold electrode (vs. Pt) in a stepwise manner from –0.5 V to +0.4 V while measuring the steady state fluorescence[5] in order to evaluate the "voltage response" of the DNA layer. A representative fluorescence trace as a function of electrode voltage of a DNA-trisNTA layer measured after Ni loading is shown in Figure S 2A. We term the inflection point of the transition region (–0.2 V to +0.2 V in Fig. S2) the 'potential of conformation transition', *pct*. The switching potentials V_{max} and V_{min}, which were required for inducing lying or standing DNA conformations, were chosen in the 'plateau' regimes sufficiently positive and negative of the *pct*, respectively (cf. Fig. S2A). In case the *pct* was found to shift by more than ±50 mV during an experiment (for instance due to shifts of the electrodes' potentials of zero charge), the switching potentials were adjusted accordingly. The amplitude of the applied square wave potential was kept constant at 0.8 V.

A representative time-resolved measurement of the upward motion of a DNA-trisNTA layer is shown together with the capacitive electrode charging current in Figure S 2B. The applied square-wave AC potential was V_{min} = –0.5 V, V_{max} = +0.3 V, f = 10 kHz. The integration time for high resolution time-resolved data traces sampled at 32 ns was 3-10 min. Since the DNA switching dynamics are known to correlate strongly with the charging time of the electrochemical double layer [10], the double layer charging current was measured with an oscilloscope (Figure S 2B). Charging times were evaluated by fitting a single exponential function to the current traces, in agreement with the notion of a polarizable interface which can be represented by a simple RC equivalent circuit model.. Generally, we did not observe changes in the charging time after proteins bound to the DNA-trisNTA layer. The velocity profile of the upward DNA motion was evaluated by computing the first derivative of the time-dependent fluorescence trace ($v_F=\partial F/\partial t$) and smoothing the v_F data with an FFT filter (f_{cutoff} = 780 kHz).

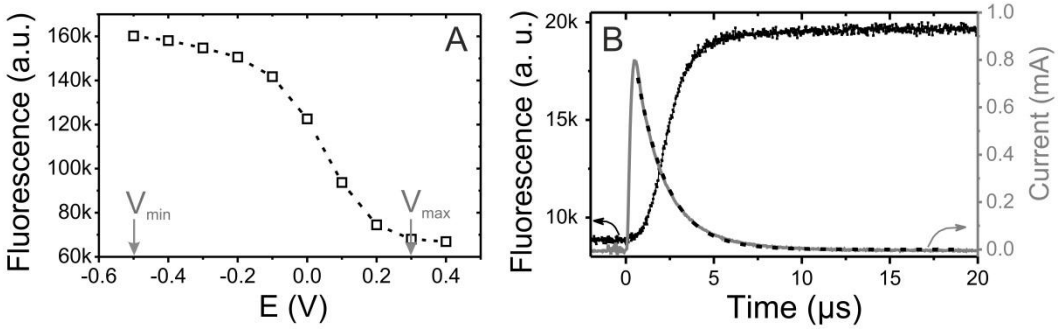

Figure S 2 Steady state and time-resolved response of a DNA-trisNTA layer. **A**: Steady state fluorescence intensity as a function of applied electrode potential (vs. Pt). V_{min} and V_{max} denote negative and positive potentials which are required for inducing standing and lying conformations of the DNA-trisNTA layer, respectively. **B**: Time-resolved measurement of the upward motion of a DNA-trisNTA layer (black symbols). At t=0 µs, the potential is switched from positive (+0.3 V) to negative (-0.5 V) values (repetition frequency f = 10 kHz). Data were sampled at 32 ns, the total integration time was 3 min. The right y-axis depicts the double layer charging current (gray line). The dashed line is a single exponential function, yielding a capacitive charging time of 1.7 µs.

1.6 Titration protocol and analysis of 'fraction bound'

DNA-trisNTA layers and reference DNA layers (without trisNTA) were simultaneously exposed to the His_6-protein solution of a given concentration. Before and after every binding experiment, the layers were characterized by steady-state and time-resolved fluorescence measurements, and the electrode charging currents were recorded. In order to minimize the unwanted dissociation of Ni^{2+} ions from trisNTA chelators ('bleeding'), DNA-trisNTA layers were either regenerated as described above or freshly prepared layers were used for every protein concentration.

The binding of proteins is analyzed from the relative change of the DNA upward velocity before and after protein binding:

[5] The fluorescence integration time was in the range of milliseconds (integration time >> DNA layer rise time ~µs).

$$v_{rel} = \frac{v_F^{max}\ (after\ protein\ binding)}{v_F^{max}\ (before\ protein\ binding = bare\ DNA)} \qquad \text{Eq. S 1}$$

As proteins bind to the DNA-trisNTA layer, the relative velocity decreases (v_{rel}<1). At sufficiently high protein concentrations ($c \to \infty$) all binding sites are occupied with proteins and v_{rel} reaches its minimal value. Usually, 2-3 electrodes were probed for a given protein concentration and the mean value of the individual measurements was evaluated ($\overline{v_{rel,trisNTA}}$ and $\overline{v_{rel,ref}}$). The velocity change upon protein binding is:

$$\Delta v_{rel} = \overline{v_{rel,ref}} - \overline{v_{rel,trisNTA}} \qquad \text{Eq. S 2}$$

The *fraction bound* value for a given protein concentration c is calculated from:

$$fraction\ bound\ (c) = \frac{\Delta v_{rel}(c) - \Delta v_{rel}(c=0)}{\Delta v_{rel}(c\to\infty) - \Delta v_{rel}(c=0)} \qquad \text{Eq. S 3}$$

Fraction bound is 0 when no protein is bound (= bare DNA) and 1 when all trisNTA binding sites are saturated with protein.

We investigated binding affinity of His_6 tagged protein A featuring two affinity tags (C- and N-terminal His6 tags) and His6 tagged protein G featuring one affinity tag (at N-terminal) to trisNTA functionalized DNA layer. Equilibrium binding isotherms of protein G is analyzed by using Langmuir model:

$$R_{eq} = \frac{c \cdot R_{max}}{c + K_d} \qquad \text{Eq. S 4}$$

where *Req* denotes equilibrium response, *Rmax* denotes maximal (saturation) response, *Kd* denotes the equilibrium dissociation constant and *c* denotes protein concentration.

The shallow progression of protein A binding curve is fitted as a linear combination of two Langmuir isotherms:

$$R_{eq} = A \cdot \frac{c \cdot R_{max}}{c + K_{d,2}} + (1 - A) \cdot \frac{c \cdot R_{max}}{c + K_{d,2}} \qquad \text{Eq. S 5}$$

2 Quantitation of association and dissociation rate constants k_{on} and k_{off}

In order to quantify the association rate constant of His_6-protein A to the trisNTA chelator, DNA-trisNTA layers were exposed to 50 nM His_6-protein A solution, while observing changes in the maximal switching velocity in real-time. Note that a concentration of 50 nM is sufficient to saturate the DNA-trisNTA layer, as shown by the titration experiment (Figure 2). For all kinetics measurements, the frequency of the *ac* potential was 60 kHz. At high driving frequency, many switching cycles are performed in a short period of time, which improves the signal to noise ratio (S/N) and enables the measurement of very fast on-rate kinetics, which occur within seconds.

Two factors can cause a decrease in the DNA-lever switching velocity: (i) an increase of the hydrodynamic drag due to protein binding and (ii) a change of the double layer charging time [5] . In order to exclude factor (ii), the double layer charging was routinely recorded with an oscilloscope (as described in 1.5). Since changes in the double layer charging time were not observed, changes in the DNA lever switching velocity could be attributed to the successive binding of His_6-tagged proteins to the DNA-trisNTA layer.

Influence of the analyte solution flow rate

Before quantitatively analyzing binding kinetics from real-time measurements, attention has to be paid to the flow rate conditions at which the experiment was conducted. Depending on the diffusivity of the analyte, the flow rate of the analyte solution, and the chemical reactivity of the analyte, the observed kinetics can be limited by mass transport (diffusion and convective flow), or the chemical reaction rate [11]. Two limiting cases can be discriminated: (i) “fast” chemical reactions of the surface-ligands with the solute

analyte molecules create a concentration depletion zone above the sensor surface and the kinetics are limited by mass transport across this depletion zone. (ii) For "slow" reactions, the analyte concentration above the sensor stays the same as in the bulk solution and the kinetics are limited by the chemical reaction. In order to analyze the chemical nature of a molecular interaction, the biosensing experiment must be performed in the reaction-limited regime. This can, in principle, be achieved by pumping the analyte solution rapidly across the surface, to provide for sufficient mass transport.

The Damkohler number (Da) is describes the ratio of the reaction rate and the mass transport rate.

$$\boldsymbol{Da} = \frac{\textbf{reaction rate}}{\textbf{mass transport rate}} \qquad \text{Eq. S 6}$$

If Da<<1, the reaction rate is much slower than mass transport, thus, the kinetics are reaction limited. For Da>>1, kinetics are governed by the mass transport rate. For rectangular channels, the Damkohler number is [11]:

$$Da = \frac{k_{on} \cdot b_m \cdot \delta}{D} = \frac{k_{on} \cdot b_m \cdot L}{D \cdot \mathcal{F}} \qquad \text{Eq. S 7}$$

where k_{on} is the association rate binding constant, b_m is the surface concentration of the targets, δ is thickness of the depletion zone, L is the length of the sensor, D is the diffusion constant, and $\mathcal{F}$ is a dimensionless flux. For extremely fast flow, it can be approximated [11]:

$$\mathcal{F}\ (Pe_s \gg 1) \sim Pe_s^{\frac{1}{3}} = \left[6 \cdot \left(\frac{L}{H}\right)^2 \cdot \frac{Q}{D \cdot W_c}\right]^{1/3} \qquad \text{Eq. S 8}$$

where Pe_s denotes the Peclet number under shear rate conditions, W_c is the width of the channel, Q is the volumetric flow rate. The diffusion coefficient can be calculated from the Einstein-Stokes equation:

$$D = \frac{k_B \cdot T}{6 \cdot \pi \cdot \eta \cdot R_H} \qquad \text{Eq. S 9}$$

where k_B ist the Bolzmann constant, T is the temperature, η is the viscosity of the solvent, and R_H is the hydrodynamic radius of the protein. The hydrodynamic diameter of His_6-protein A was measured by dynamic light scattering to be D_H = (6.7 ± 0.9) nm. The typical surface density of the DNA-trisNTA layer and hence density of protein binding sites is assumed to be 5 x 10^{10} molecules/cm² ≈ 83 fmol/cm² [4]. The association rate constant of His_6-tagged proteins to trisNTA is expected to be <10^6 $M^{-1}s^{-1}$ (Table S 2).

Hence, Table S 1 lists the calculated Damkohler numbers for different analyte flow rates for the present experimental situation.

Table S 1 Damkohler numbers calculated for His_6-protein A and used sensor design at different volumetric flow rates.

Volumetric flow rate (ml/min)	Da
0.5	0.10
1	0.09
2	0.07
5	0.05

For our experiments, Da<<1. Thus, the binding kinetics of His_6-protein A are expected to be reaction limited for volumetric flow rates 0.5-5 ml/min.

In order to experimentally verify that the observed association rates are governed by the chemical reaction, the binding of His_6-protein A to DNA-trisNTA layers was investigated for different flow rates. Time constants which were evaluated from single exponential fits to the association phase are shown in Figure S 3. Even though the flow rate was varied over one order of magnitude, the on-rate time constant remained constant. Thus, we conclude that for all investigated flow rates the observed association rates in fact reflect the chemical reaction rates and are not limited by mass-transport.

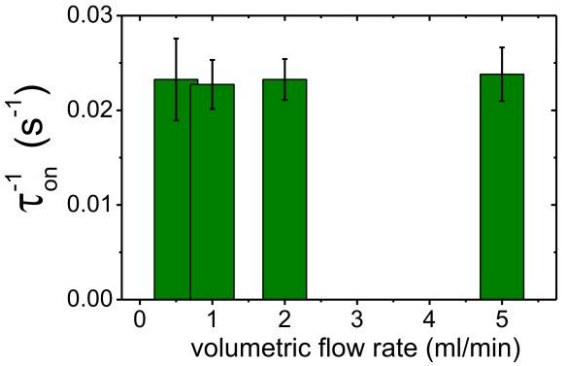

Figure S 3 Influence of the flow rate on the binding kinetics of His_6-protein A. Error bar are standard deviations of the numerical fit.

Association rate

The association kinetics were analyzed by first order binding kinetics. trisNTA chelator and His_6-proteins bind in a 1:1 stoichiometric ratio [12, 13]. The observed association rat reflects influences of association of analyte to the ligand, as well as dissociation of the analyte from the ligand:

$$\frac{\mathbf{d}}{\mathbf{dt}}\mathbf{R_t} = \mathbf{k_{on}} \cdot \mathbf{c} \cdot (\mathbf{R_0} - \mathbf{R_t}) - \mathbf{k_{off}} \cdot \mathbf{R_t} \qquad \text{Eq. S 10}$$

R_t denotes the measured signal response at time t, (R_0-R_t) corresponds to number of free binding sites, c is the target concentration, k_{on} is the association rate constant, and k_{off} is the dissociation rate constant. Solving the differential equation, we obtain

$$\mathbf{R_t} = \frac{\mathbf{k_{on} \cdot c \cdot R_0}}{\mathbf{k_{on} \cdot c + k_{off}}} \cdot \left[\mathbf{1} - \mathbf{e}^{(-(\mathbf{k_{on} \cdot c + k_{off}}) \cdot \mathbf{t})}\right] = \frac{\mathbf{k_{on} \cdot c \cdot R_0}}{\boldsymbol{\tau}_{\mathbf{on}}} \cdot \left(\mathbf{1} - \mathbf{e}^{\left(-\frac{\mathbf{t}}{\boldsymbol{\tau}_{\mathbf{on}}}\right)}\right) \qquad \text{Eq. S 11}$$

with the association time constant

$$\boldsymbol{\tau}_{\mathbf{on}}^{\mathbf{-1}} = \mathbf{k_{on}} \cdot \mathbf{c} + \mathbf{k_{off}} \qquad \text{Eq. S 12}$$

Binding experiments were repeated for different concentrations of His_6-protein A (5, 20, 50, 100, and 200 nM). The association time constant as a function of protein concentration is shown in Figure S 4. The association time constant is a linear function of the target concentration, thus the association and dissociation rate constants can be evaluated as the slope and the y-axis intercept, respectively (Eq. S 13). For His_6-protein A we obtained an association rate constant k_{on} = (4.7 ± 0.3) x 10^5 M^{-1} s^{-1}. If the dissociation rate is very low ($k_{off} << k_{on}$) like here, an estimation of the dissociation rate constant from the association phase (i.e. the intercept of the y axis) is not accurate.

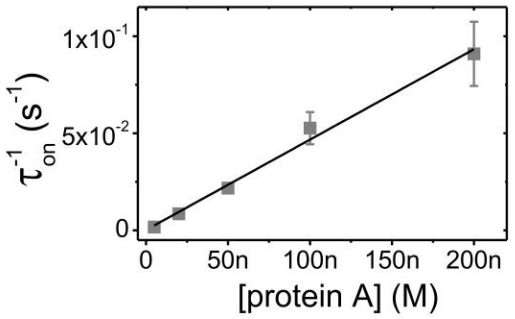

Figure S 4 Linear dependency of the association time constant on the analyte (His_6-protein A) concentration. The solid line is a linear fit with Eq. S 12 $\tau_{on}^{-1} = k_{on} \cdot c + k_{off}$. Error bars are the standard deviations of the fit.

Dissociation rate

The dissociation rate constant is analyzed by real-time monitoring of the ligand–analyte dissociation in buffer solution. In order to avoid rebinding of the dissociated His_6-protein A, buffer solution is flowed at a high flow rate (2 ml/min) across the sensor surface. The dissociation of His_6-protein A from a DNA-trisNTA layer is shown in Figure 3 (green triangles). Opposite to the case of protein binding, the dissociation of proteins correlates entails a decrease in hydrodynamic drag and, consequently, an increase of the DNA layer switching velocity. In standard buffer (50 mM NaCl, 10 mM Tris, pH 7.4), we observed a very slow dissociation of His_6-protein A from the DNA-trisNTA layer. After approximately 3.5 h of continuous rinsing with buffer, only 10% of His_6-protein A dissociated from the DNA-trisNTA layer. Since DNA-trisNTA binds 1:1 to the His_6-proteins [12, 13], the dissociation phase can be described as:

$$\frac{d}{dt}R_t = -k_{off} \cdot R_t \;\Rightarrow\; R_t \propto e^{-k_{off} \cdot t} \qquad \text{Eq. S 13}$$

The dissociation rate constant was evaluated from fitting the single exponential Eq. S 14 to the data: k_{off} = (1.1 ± 0.9) x 10^{-4} s^{-1}. This value is in good agreement with the dissociation rate constant calculated from the titration $K_{D,1}$-value and the association rate: $k_{off} = k_{on} \cdot K_{D,1}$ = 0.4 x 10^{-4} s^{-1}. Both binding rate constants are in good agreement with the literature, where association rate constants between 10^5 – 10^6 $M^{-1}s^{-1}$ and dissociation rate constants between 10^{-4} – 10^{-2} s^{-1} are reported (Table S 2).

Dissociation in the presence of competitor

We investigated the influence of a competitor (imidazole) on the dissociation rate constant of His_6-protein A from DNA-trisNTA layers. DNA-trisNTA layers were saturated with His_6-protein A (50 nM) and subsequently exposed to different concentrations of imidazole.. Representative dissociation curves in 0, 0.2 mM, 1 mM, and 100 mM imidazole solutions are shown Figure 3B. The amount of protein bound to the DNA-trisNTA layer was quantified after exposing the layers to imidazole solutions for 10 min (Figure 3C). The half maximal effective concentration EC_{50} = (1.8 ± 0.5) mM was evaluated from fitting the sigmoidal function with variable slope

$$\mathbf{R} = \frac{\mathbf{R_{max}}}{\mathbf{1}+\left(\frac{\mathbf{c_{imidazole}}}{\mathbf{EC_{50}}}\right)^{\mathbf{p}}} \qquad \text{Eq. S 14}$$

R denotes measured signal response, R_{max} is the maximal signal response, $c_{imidazole}$ is the imidazole concentration, and p is the Hill slope.

Full dissociation of the His_6-protein A from the DNA-trisNTA layer was observed at 30 mM imidazole, which is in good agreement with results obtained by Lata et al. [14], who investigated the interaction of a cyclic trisNTA chelator with His_6-tagged maltose binding protein by size exclusion chromatography and observed elution in 20 mM imidazole.

3 Association and dissociation curves of His_6-tagged proteins

The binding properties of histidine tags depend on various factors, for instance, the accessibility of the tag which might be partly 'buried' within the folded protein, or the chemical nature (e.g. charge) of the protein surface in the proximity of the tag. In order to investigate the influence of the individual nature of different proteins on the ability of their His_6-tag to bind to a trisNTA chelator, we compared the binding kinetics of six different proteins. By using a volumetric flow rate of 1 ml/min, the sensor was operated in the reaction-limited regime. DNA-trisNTA layers and reference layers were simultaneously exposed to 50 nM His_6-protein solution.

Association curves of His_6-interferon alpha (INFα), His_6-protein L, His_6-protein G, His_6-myelin oligodendrocyte glycoprotein (MOG), and of His_6-Fab fragment (Fab) are shown in Figure S 5, The high stability of the trisNTA-His_6 interaction (k_{off}~10^{-4} s^{-1}) makes a precise determination of the dissociation rate constant time consuming. Thus, the dissociation was facilitated by 10 mM imidazole. The dissociation curves are shown in Figure S 5.

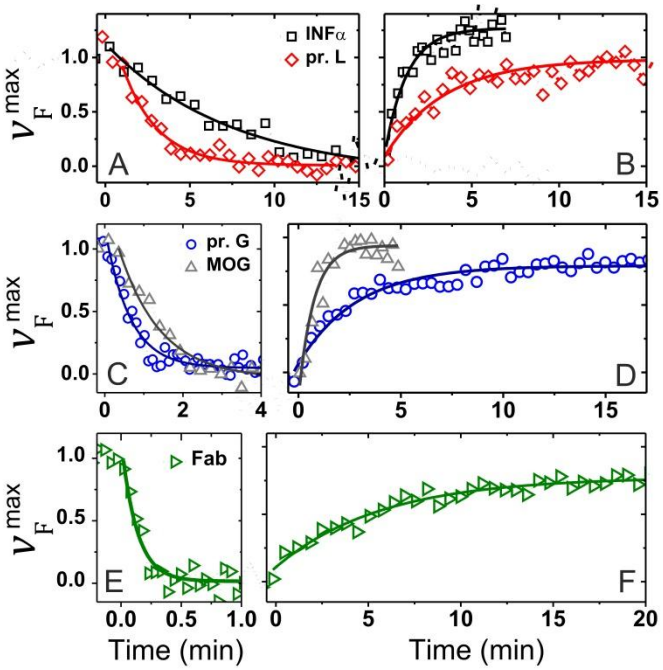

Figure S 5 Association and dissociation kinetics of different His_6-tagged proteins. The maximal switching velocity v_F^{max} of the DNA-trisNTA layer was observed in real-time while the layer was exposed to 50 nM -protein solutions at time t=0 (panels A, C and E). Subsequently, dissociation was induced by 10 mM imidazole (panels B, D and F). Association curves of interferon alpha (INFα) and protein L are shown in panel A, of protein G and myelin oligodendrocyte glycoprotein (MOG) in panel C, and of Fab in panel E. Dissociation curves of INFα and protein L are shown in panel B, of protein G and MOG in panel D, and of Fab in panel F. Solid lines are single exponential fits.

Very different association and dissociation kinetics were observed for the six investigated His_6-proteins. While binding of INFα takes 15 min (Figure S 5A, black rectangles), the trisNTA ligands become saturated with Fab in only 35 s (Figure S 5E). In the presence of 10 mM imidazole, it takes only 3 min for INFα to completely dissociate from the trisNTA ligands (Figure S 5B, black rectangles), yet, even after 20 min, only 75% of the His_6-tagged Fab dissociated Figure S 5F). The reference layers showed no response in the in the presence of His_6-protein solutions (Figure S 6), confirming the specificity of the His_6–trisNTA interaction.

Rate constants were analyzed by fitting single exponential functions to the data (solid lines in Figure S 5). Since $k_{on} \times c \approx 2.2 \cdot 10^{-2}\ s^{-1} \gg 1 \cdot 10^{-4}\ s^{-1} \approx k_{off,buffer}$ (as shown for His_6-protein A), we approximate:

$$\boldsymbol{\tau_{on}^{-1} = k_{on} \cdot c + k_{off} \approx k_{on} \cdot c} \qquad \text{Eq. S 15}$$

All analyzed binding rate constants are summarized in Table S 2. The association rates varied from 0.4 x 10^5 $M^{-1}s^{-1}$ (for INFα) to 26 x 10^5 $M^{-1}s^{-1}$ (for Fab). In the literature, association rate constants between 10^5 – 10^6 $M^{-1}s^{-1}$ were reported (Table S 2, [1, 12-15]). Huang et al. [15] observed variations of the association rate constants for six different His_6-proteins over one order of magnitude. The dissociation rates (in 10 mM imidazole solution) varied over one order of magnitude.

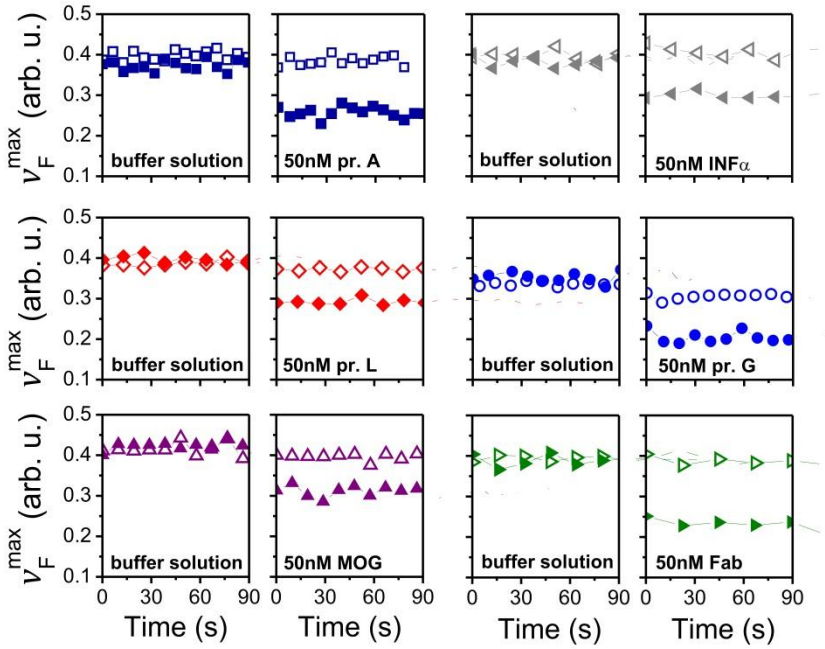

Figure S 6 Maximal switching velocities of DNA-trisNTA and reference layers (DNA without trisNTA) in buffer and in 50 nM His_6-protein solutions. Empty symbols depict reference layers and solid symbols DNA-trisNTA layers.

Table S 2 Experimental and published kinetic rate constants (k_{on}, k_{off}) and dissociation constants (K_D) of His_6-tagged proteins binding to trisNTA ligands.

Protein	k_{on}	k_{off}	k_{off}*	$K_D=k_{off}/k_{on}$	K_D	Method	Probe	trisNTA scaffold	Ref.
	10^5 $M^{-1}s^{-1}$	10^{-3} s^{-1}	10^{-3} s^{-1}	nM	nM				
INF-alpha	0.4 ± 0.1	n/a	13 ± 2	n/a	n/a	Time-resolved DNA switching, *switch*SENSE	ds48-DNA-trisNTA	linear	this work
MOG	3.1 ± 0.4	n/a	22 ± 5	n/a	n/a				
Fab	26 ± 7	n/a	2.9 ± 0.4	n/a	n/a				
protein A	4.9 ± 0.5	0.11±0.09	7.5 ± 0.8	0.2 ± 0.2	0.91 and 1.5				
protein G	5.3 ± 0.6	n/a	5.8 ± 0.6	n/a	6.1 ± 0.3				
protein L	1.6 ± 0.2	n/a	4.9 ± 0.6	n/a	n/a				
GFP	n/a	n/a	n/a	n/a	6	FRET	trisNTA-27ssDNA-Cy3		[1]
MBP	n/a	n/a	n/a	n/a	20	ITC[(i)]	trisNTA	cyclic	[12]
peptide	1.6	0.34	n/a	2.1	n/a	TRFS[(ii)]	carboxyfluorescein-trisNTA		
MBP	1.0-5.0	0.3	n/a	<5	<5	FRET[(iii)]	Oregon Green 488-trisNTA		[14]
HIP1R	0.9-1.9	2.9-4.3	n/a	18-33	n/a	SPR[(iv)]	biotin-trisNTA on SA chip		[13]
yCD	4.1	2.2	n/a	5.4	n/a				
AR-NTDa, yCDb, TSG6c, peptided, and mKatee	1.0-35	0.01-12	n/a	0.02-40	n/a	SPR	biotin-trisNTA on SA chip		[15]

[(i)]Isothermal Titration Calorimetry, [(ii)]Time-Resolved Fluorescence Spectrometry, [(ii)]Fluorescence Resonant Energy Transfer, [(iv)]Surface Plasmon Resonance
[a]Androgen receptor N-terminal domain, [b]Yeast cytosine deaminase, [c]Tumor necrosis factor R-stimulated gene-6, [d]GWGGHHHHHHG, [e]Monomeric Katushka, a far-red fluorescent protein

4 SPR (Biacore) reference measurements

In order to validate the substantial differences in binding kinetics and affinities that were observed for different His6-tagged proteins with the switching method, we performed reference measurement with the Biacore™ X100 (General Electric) surface plasmon resonance (SPR) system. A commercially available "Sensor Chip NTA" from GE was used and standard protocols as suggested by the manufacturer in the "NTA reagent kit" were applied. Note that, contrary to the trisNTA capture probes used in the switching experiments, the NTA sensor chip features monovalent NTA groups. Thus, absolute binding affinities are not comparable, but relative differences in the binding parameters of different proteins should also be observable in the SPR measurement.

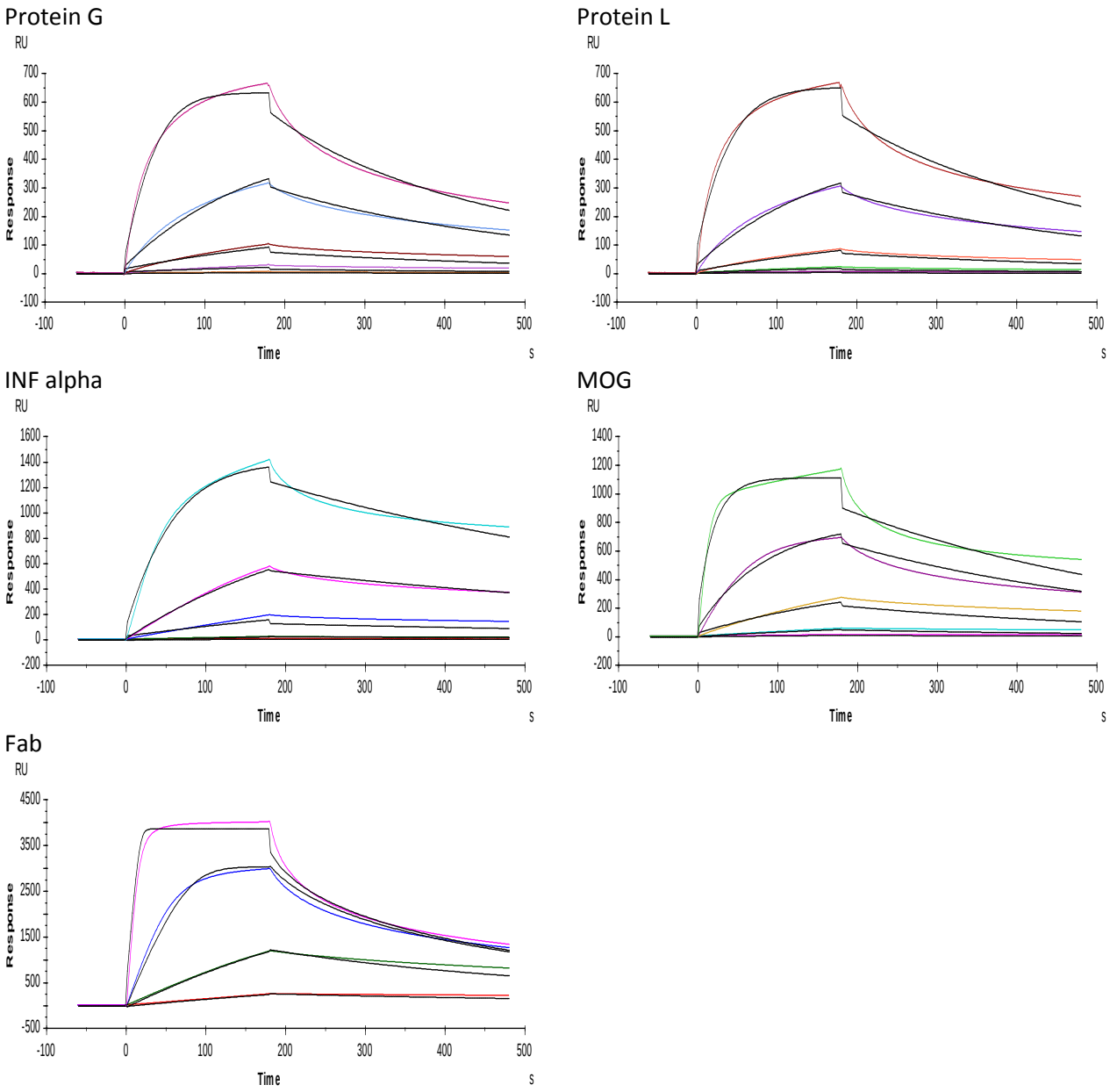

Figure S 7 Surface plasmon resonance sensorgrams of His_6-tagged proteins binding to a Biacore NTA sensor chip (monovalent NTA) in HBS-P+ buffer (0.01M HEPES, 0.15M NaCl, 0.005% surfactant P20, pH 7.4) with 50 µM EDTA. Proteins were

injected at concentrations of 2.4 nM, 12 nM, 60 nM, 300 nM, 1500 nM in 30 µl/min flow. In between injections, the NTA chip was regenerated with 350 mM EDTA in HBS-P+ (pH 8.3) and subsequently exposed to a 0.5 mM $NiCl_2$ HBS-P+ solution for Nickel-loading. Data were fitted globally with a 1:1 interaction model (Langmuir), fits are shown as black lines.

SPR sensorgrams for the 5 investigated proteins with one His_6-tag are shown in Figure S7. Data were analyzed with a 1:1 interaction model using the 'Biacore X100 Evaluation Software' package. Although rated 'good' by the software, we note that the quality of the global fits (accounting for all concentrations at once), is not very satisfying. Individual fitting of single concentrations yielded better agreement between data and model, but significant discrepancies for the interaction parameters determined for different concentrations were obtained. Nevertheless, for the sake of comparing differences in the interaction parameters between different proteins, the results of the global fit were used and are summarized in Table S3.

In agreement with the switching data, the SPR results show substantial differences in the interaction parameters of different proteins. As for the switchSENSE values, SPR k_{on} values vary by two orders of magnitude (1.35 – 153 x 10^4 $M^{-1}s^{-1}$), and k_{off} values vary by one order of magnitude (1.6 – 12 x 10^{-3} s^{-1}).

Table S 3 Interaction parameters of His_6-tagged proteins with a "Sensor chip NTA" (monovalent NTA), determined with the Biacore X100 SPR system.

Protein	**R_{max} (RU)**	**k_{on} (10^4 $M^{-1}s^{-1}$)**	**k_{off} (10^{-3} s^{-1})**	**K_D (nM)**
Protein G	631	2.63	4.25	162
Protein L	623	2.03	3.41	168
INF alpha	1385	1.35	1.57	117
MOG	951	3.02	2.41	79.8
Fab	3483	153.8	12.24	8.0

5 Protein-protein interaction

In order to demonstrate the capability of using the method for a protein-protein interaction assay, we tested whether a secondary protein could be bound to a primary His_6-tagged protein. Figure S8 shows the upward switching velocity profile of a trisNTA modified DNA layer before binding the primary protein, after capturing His_6-tagged protein L as the primary protein, and after incubation with a monoclonal mouse IgG_1 (Clone B25, AbD Serotec, Germany) antibody as the secondary protein. Protein L is known to bind mouse IgG antibodies via their Fab fragments. As expected, the maximal velocity decreased after capturing protein L and – even more significantly – after incubation with the large (150 kDa) IgG. Evidently, the protein L – IgG interaction can be detected by the switchSENSE method.

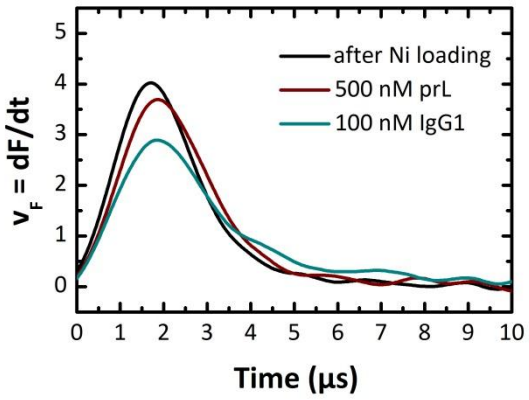

Figure S 8 Upward switching velocity (cf. Figure 1 in the main paper) profile upon successive binding of His_6-tagged protein L and a monoclonal mouse antibody (IgG_1) to a trisNTA modified DNA layer.

6 References

1. Goodman, R.P., et al., *A Facile Method for Reversibly Linking a Recombinant Protein to DNA.* ChemBioChem, 2009. **10**(9): p. 1551-1557.
2. Arinaga, K., et al., *The Role of Surface Charging during the Coadsorption of Mercaptohexanol to DNA Layers on Gold: Direct Observation of Desorption and Layer Reorientation.* Langmuir, 2006. **22**(13): p. 5560-5562.
3. Herne, T.M. and M.J. Tarlov, *Characterization of DNA Probes Immobilized on Gold Surfaces.* Journal of the American Chemical Society, 1997. **119**(38): p. 8916-8920.
4. Arinaga, K., et al., *Controlling the surface density of DNA on gold by electrically induced desorption.* Biosensors and Bioelectronics, 2007. **23**(3): p. 326-331.
5. Rant, U., et al., *Dynamic Electrical Switching of DNA Layers on a Metal Surface.* Nano Letters, 2004. **4**(12): p. 2441-2445.
6. Steel, A.B., T.M. Herne, and M.J. Tarlov, *Electrochemical Quantitation of DNA Immobilized on Gold.* Analytical Chemistry, 1998. **70**(22): p. 4670-4677.
7. Ulrich Rant , K.A., Simon Scherer, Erika Pringsheim, Shozo Fujita, Naoki Yokoyama, Marc Tornow, and Gerhard Abstreiter, *Switchable DNA interfaces for the highly sensitive detection of label-free DNA targets.* PNAS, 2007. **104**(44): p. 17364-17369.
8. Kågedal, L., *Immobilized Metal Ion Affinity Chromatography*, in *Protein Purification*. 2011, John Wiley & Sons, Inc. p. 183-201.
9. Tareste, D., et al., *The Binding Energy of Two Nitrilotriacetate Groups Sharing a Nickel Ion.* Journal of the American Chemical Society, 2005. **127**(11): p. 3879-3884.
10. Rant, U., ed. *Electrical manipulation of DNA-layers on gold surfaces*. 1, from 6. März 2006 ed. 2006, Verein zur Förderung des Walter Schottky Instituts der Technischen Universität München.
11. Squires, T.M., R.J. Messinger, and S.R. Manalis, *Making it stick: convection, reaction and diffusion in surface-based biosensors.* Nat Biotech, 2008. **26**(4): p. 417-426.
12. Lata, S., et al., *High-Affinity Adaptors for Switchable Recognition of Histidine-Tagged Proteins.* Journal of the American Chemical Society, 2005. **127**(29): p. 10205-10215.
13. Huang, Z., et al., *Facile Synthesis of Multivalent Nitrilotriacetic Acid (NTA) and NTA Conjugates for Analytical and Drug Delivery Applications.* Bioconjugate Chemistry, 2006. **17**(6): p. 1592-1600.
14. Lata, S., et al., *Specific and Stable Fluorescence Labeling of Histidine-Tagged Proteins for Dissecting Multi-Protein Complex Formation.* Journal of the American Chemical Society, 2006. **128**(7): p. 2365-2372.
15. Huang, Z., et al., *Tris-Nitrilotriacetic Acids of Subnanomolar Affinity Toward Hexahistidine Tagged Molecules.* Bioconjugate Chemistry, 2009. **20**(8): p. 1667-1672.